

IN-34  
394 661

# NASA

## MEMORANDUM

HEAT TRANSFER FROM A HORIZONTAL CYLINDER ROTATING IN OIL

By R. A. Seban and H. A. Johnson

University of California

NATIONAL AERONAUTICS AND  
SPACE ADMINISTRATION

WASHINGTON

April 1959



NATIONAL AERONAUTICS AND SPACE ADMINISTRATION

MEMORANDUM 4-22-59W

HEAT TRANSFER FROM A HORIZONTAL CYLINDER ROTATING IN OIL

By R. A. Seban and H. A. Johnson

SUMMARY

Measurements of the heat transfer from a horizontal cylinder rotating about its axis have been made with oil as the surrounding fluid to provide an addition to the heat-transfer results for this system heretofore available only for air. The results embrace a Prandtl number range from about 130 to 660, with Reynolds numbers up to  $3 \times 10^4$ , and show an increasing dependence of free-convection heat transfer on rotation as the Prandtl number is increased by reducing the oil temperature. Some correlation of this effect, which agrees with the prior results for air, has been achieved.

At higher rotative speeds the flow becomes turbulent, the free-convection effect vanishes, and the results with oil can be correlated generally with those for air and with mass-transfer results for even higher Prandtl numbers. For this system, however, the analogy calculations which have successfully related the heat transfer to the friction for pipe flows at high Prandtl numbers fail.

INTRODUCTION

The transfer of heat from a horizontal cylinder rotating about its axis in an environment of ambient air has been measured and reported in references 1 to 4. Consequently, the heat-transfer coefficient for this system has been defined for Reynolds numbers up to  $4.3 \times 10^5$  and for Grashof numbers from  $1 \times 10^5$  to  $8 \times 10^6$ . The salient features emerging from these measurements are the relative insensitivity of the free-convection performance to rotation before transition and the primary dependence of heat transfer on rotation after transition to turbulence. After transition the Grashof number, which decays rapidly as the heat transfer increases, has an almost negligible effect on the heat transfer. For the turbulent region, the heat-transfer coefficient is specified fairly well by the relation proposed by Etemad (ref. 2):

$$\frac{hd}{k} = 0.076 \left( \frac{ud}{\nu} \right)^{0.70} \quad (1)$$

By using the friction coefficients as found by Theodorsen (ref. 5), the above equation gives Nusselt numbers slightly higher than those predicted by the Colburn relation

$$\frac{hd}{k} = \frac{c_f}{2} \left( \frac{ud}{\nu} \right) \left( \frac{\nu}{\alpha} \right)^{1/2} \quad (2)$$

Applications of analogies between heat and momentum transfer of the Karman type have been made by Mayhew (ref. 6) and Kays (ref. 3) to show that the heat-transfer coefficients can be predicted from the friction in this way also. For Prandtl numbers near unity, this is to be expected from the applicability of equation (2), but the relative success of the Karman analogy rests too on the diminished effect of free convection, which must of course be neglected in the analogy calculation. With turbulent flow the region of free convection moves away from the cylinder surface and the heat is thus carried into the surrounding air with a relatively small temperature difference, as is evident from the temperature profiles obtained by Anderson (ref. 1) and Kays (ref. 3).

Eisenberg (ref. 7) obtained mass-transfer results for rotating cylindrical electrodes and provided Schmidt numbers in the range from 8,000 to 12,000, with Reynolds numbers from 200 to  $10^5$ . The density variation was negligible, so that there were no free-convection effects and the best correlation of results was obtained by a relation similar to equation (2). Cast into the form of a heat-transfer equation, the correlation is

$$\frac{hd}{k} = \frac{c_f}{2} \frac{ud}{\nu} \left( \frac{\nu}{\alpha} \right)^{0.356} \quad (3)$$

With a Prandtl number of 0.70 the air results are obviously predicted as well by either equation (2) or (3).

The experiments reported here were undertaken to determine the effect of Prandtl numbers other than 0.70 on the heat-transfer performance, with particular emphasis on the free-convection region, since it could already be anticipated that equation (3) should provide a fair prediction for the region of turbulent flow. This was done by observing the performance of a horizontal cylinder rotating in oil, by which laminar free-convection flows with Grashof numbers from  $7 \times 10^3$  to  $5 \times 10^5$  and Prandtl numbers from 130 to 660 were obtained. Reynolds numbers ranged from zero to  $3 \times 10^4$  and the region of fully turbulent flow was also adequately defined.

A different range of Prandtl and Grashof numbers was realized by operation with water instead of oil. These results are presented separately in appendix A, where it is shown that they are consistent with the measurements made with oil.

Appendix B contains results on Etemad's cylinder operated vertically in air. While not directly related to the objective of the reported investigation, these results were obtained during the investigation and are presented as additional information on rotating systems.

The present investigation was conducted at the University of California under the sponsorship and with the financial assistance of the National Advisory Committee for Aeronautics. Data were obtained and results were calculated by Messrs. E. Quinn, P. Niles, and A. Levy. Technical assistance was rendered by the Division of Mechanical Engineering, University of California.

#### SYMBOLS

|            |   |
|------------|---|
| $c$        | specific heat, Btu/(lb)(°F)                               |
| $c_f$      | friction coefficient, $2\tau_o/\rho u^2$                  |
| $d$        | cylinder diameter, in.                                    |
| $Gr$       | Grashof number, $\frac{g\beta \Delta t d^3}{\nu^2}$       |
| $g$        | acceleration of gravity                                   |
| $h$        | heat-transfer coefficient, Btu/(ft <sup>2</sup> )(hr)(°F) |
| $k$        | thermal conductivity, Btu/(ft)(hr)(°F)                    |
| $Nu$       | Nusselt number, $\frac{hd}{k}$                            |
| $Pr$       | Prandtl number, $\frac{\nu}{\alpha}$                      |
| $q$        | heat flux, Btu/ft <sup>2</sup> hr                         |
| $Re$       | Reynolds number, $\frac{ud}{\nu}$                         |
| $r$        | cylinder radius, ft                                       |
| $t$        | temperature, °F   |
| $t_o$      | temperature at cylinder surface                           |
| $t_\infty$ | temperature in fluid                                      |

|                             |   |
|-----------------------------|---|
| $u$                         | peripheral velocity of cylinder surface, ft/sec |
| $x$                         | heated height, vertical cylinder, ft            |
| $\alpha$                    | thermal diffusivity, ft <sup>2</sup> /hr        |
| $\beta$                     | coefficient of thermal expansion, 1/°F          |
| $\Delta t = t_0 - t_\infty$ |   |
| $\mu$                       | viscosity of oil                                |
| $\nu$                       | kinematic viscosity, ft <sup>2</sup> /hr        |
| $\rho$                      | density of oil, lb/cu ft                        |
| $\tau$                      | skin friction, lb/sq ft                         |

#### APPARATUS AND PROCEDURE

The experimental system consisted of a 2.50-inch-diameter circular cylinder mounted horizontally in a tank having a horizontal cross section of 15 by 36 inches, the cylinder spanning the 15-inch dimension. The axis of the cylinder was 16 inches above the bottom of the tank and the fluid level was maintained at about 18 inches above the axis. In this way the shear at the fluid boundaries with two-dimensional laminar motion as produced by cylinder rotation would be less than 1/2 percent of the shear at the cylinder surface. The tank also contained electric heaters at the bottom and cooling coils on its narrow sides for the adjustment of the oil temperature. The protruding shaft of the cylinder provided a location for an external belt drive and slip rings for electric heating current and thermistor connections.

The cylinder was made of grade G-3 Phenolite with a Fiberglas base and had an inside diameter of 2 inches. Chromel ribbon 0.002 inch thick and 0.50 inch wide was wrapped helically around the cylinder in 14 closely spaced turns, leaving unheated end sections approximately  $3\frac{1}{2}$  inches long. Electrical connections were made through the rigidly held ribbon ends by wires passing within the cylinder and through the supporting shaft to the external slip rings. Thermistors and thermocouples were placed in the cylinder at various positions immediately below the ribbon, the leads passing within the cylinder to the external slip-ring assembly. Rock wool was packed into the interior of the cylinder to eliminate convection there. Figure 1 is a sketch of the elevation of the cylinder in the tank and reveals the general dimensions and the position of the ribbon on the cylinder.

Fluid temperatures were measured by thermocouples placed on vertical lines 10 inches away from the cylinder axis with junctions in the plane of the cylinder and 15 inches above and 8 inches below it. The oil was a medium (Freezone) oil having the properties shown in figure 2.

The measurements necessary for the heat-transfer determination were the steady-state values of electric current (a.c.) to the ribbon, the fluid thermocouple response, the thermistor resistance, and the rotative speed of the cylinder. From these and the known resistance of the ribbon there could be determined the heat flux and temperatures of the cylinder surface and of the fluid which were necessary for the evaluation of the heat-transfer coefficient  $h = q/(t_o - t_\infty)$ .

Surface temperatures were determined from the response of the thermistor at the center of the cylinder (location 1 in fig. 1). It was calibrated by observing the thermistor and the response of an adjacent thermocouple with the cylinder stationary and unheated and the oil agitated. The error in the temperature difference between the cylinder surface and that of the fluid, so evaluated, was no greater than  $0.5^\circ \text{F}$ .

The heat flux was evaluated directly from the electrical dissipation in the ribbon, since calculation of the longitudinal conduction based on temperatures observed in the cylinder surface revealed this to give a negligible error at the center of the cylinder. In the worst case, that of free convection to air, the amount of longitudinal conduction to the unheated ends was, at the center, less than 1 percent of the rate at which heat was generated at the center of the heated section.

In the majority of cases the temperature difference was of the order of  $20^\circ \text{F}$ , giving a possible error of less than 5 percent in the heat-transfer coefficient. This may have been exceeded in free-convection operation, where in some instances small temperature differences were used to attain low Grashof numbers. There, too, the surface temperature was evaluated as the average of the steady values obtained from observations made with the thermistor location placed successively at  $30^\circ$  intervals around the cylinder periphery.

## RESULTS

The results obtained with oil are given along with the essential operating conditions in table I and are shown graphically in figures 3 to 7 in dimensionless form in terms of the Nusselt, Reynolds, Prandtl, and Grashof numbers. These numbers have been evaluated from fluid properties taken at the film temperature, which is the arithmetic average of the surface and fluid temperatures. This choice of property evaluation is a significant factor in the consideration of any correlation

that is achieved, for the fluid viscosity varies considerably with the temperatures and other bases of property evaluation would alter materially the values of those numbers in which the viscosity is involved. The film temperature was chosen because of its success in correlating results from high Prandtl number fluids for free convection and for flow in pipes.

Figure 3 shows the results obtained with free convection from the stationary cylinder both in air and in oil, and they are compared there with the correlation equation proposed by McAdams (ref. 8):

$$\frac{hd}{k} = 0.53 \left( \frac{g\beta \Delta t d^3}{\nu^2} \frac{\nu}{\alpha} \right)^{1/4} \quad (4)$$

The comparison is favorable, the points for oil (at Grashof numbers greater than  $4 \times 10^6$ ) being within 5 percent of the values predicted by equation (4), while the values for air (those at lower Grashof numbers) are about 10 percent low. In this connection it is necessary to recall that the existing results which support equation (4) are hardly within these limits and also that equation (4) refers to constant surface temperature, while in the present system the heat flux approached a constant value around the periphery.

Figure 4 presents a part of the results obtained with the cylinder rotating in oil and demonstrates in particular the effect of rotation on the free-convection performance. There the group  $\frac{hd}{k} \left( \frac{\alpha}{\nu} \right)^{1/4}$  is plotted against the Reynolds number, so that for free convection alone the ordinate should depend only on the Grashof number, according to equation (4). It was impossible, however, to control the experimental system in such a way that constant Grashof numbers were obtained at the various speeds, thus only the order of magnitude was maintained and the orders of the Grashof and Prandtl numbers reflected by the different point designations are indicated in the figure. Also, the corresponding free-convection values are shown by points on the ordinate scale. It is evident that the effect of rotation is extremely variable and is in some way dependent on both the Grashof and Prandtl numbers when the Reynolds number is low and free convection predominates. At lower Prandtl numbers, like 138, the effect of rotation is small and the magnitude of the heat-transfer coefficient typical of free convection is preserved almost to the point of transition to turbulent flow. Conversely, at the high Prandtl number of 660, there is a radical decrease in the heat-transfer coefficient as the rotative speed increases. After the transition to turbulent flow, as indicated by the independence of the Grashof number achieved at the higher speeds, figure 4 shows that there is some correlation of results. This point is discussed later and here it is observed only that synthesis of the kind of results shown in figure 4 is possible only by separate



consideration of the regions of predominating free convection, of transition, and of turbulent flow.

### Free-Convection Region

The free-convection region is considered to embrace Reynolds numbers up to the point of the minimum Nusselt number; it is the region of greatest randomness in the representation of figure 4. An obvious alternative to the representation used there is the specification of the ratio between the observed heat-transfer coefficient and the value given for it by equation (4) in order to obtain a ratio indicating the change in the heat-transfer coefficient due to rotation. It is the appropriate representation of this ratio that is difficult to establish. Analysis is the obvious source for such a relation but it cannot be made directly fruitful because of the complexity of the system considered. If integral methods are used, the velocity distribution in the boundary layer can be taken in a way that accounts for cylinder rotation, but the introduction of such a velocity distribution and of an appropriate temperature distribution does not lead to the kind of initial-value problem that exists, for instance, for the stationary cylinder as formulated by Levy (ref. 9). The form of the ordinary differential equations so obtained does, however, suggest that the ratio of the heat-transfer coefficients might depend on a group such as  $RePr/\sqrt{GrPr}$ . Figure 5 shows all the results on this basis, all the points from zero speed up to and including the minimum Nusselt number being included. There still exists too much dispersion to claim a relation, but, contrasted with some other empirical attempts, the representation of figure 5 affords the best grouping of the results so far obtained. At abscissa values less than 3, particularly, there is considerable scatter with a number of ordinates exceeding unity. This infers that with low relative rotational speeds there may be at first a slight increase in the heat transfer. Such a deduction is hardly justified by the scatter of the points in this region and therefore at present the region of  $RePr/\sqrt{GrPr} < 3$  is considered to be one where rotation has negligible influence on the free-convection heat transfer.

In addition to providing a rationalization of the observations made with oil, the representation of figure 5 is in agreement with most of the available results for air and those for water as contained in appendix A. All the results for air available in the free-convection region have values of  $RePr/\sqrt{GrPr} < 2$ , so that figure 5 would indicate negligible effect of rotation on free convection and this is indeed the case. For water this is true in a similar way.

## Transition

If figure 5 is used to deduce the effect of rotation on the heat transfer, then reasonable results will be obtained provided that transition to turbulent flow does not occur. The appraisal of this transition must be made separately and at present on a basis even more empirical than that of the free-convection region. Anderson (ref. 1) examined his results for air and was led to the estimate that transition would occur when the peripheral velocity of the cylinder was equal to the maximum free-convection velocity that would exist on the cylinder if it were stationary. Thus he specified for the transition Reynolds number the value  $0.53\sqrt{Gr/Pr}$  and found this to be in good agreement with his observations. This is, however, wholly inconsistent with the present results for oil.

The rather arbitrary nature of Anderson's assumption becomes defensible immediately upon a search for an alternate specification, and it becomes necessary to rely on the direct observation that, upon attainment of the turbulent regime, the heat-transfer coefficient has a value practically the same as that for the stationary cylinder. Then the Nusselt numbers of equations (4) and (2) can be equated (eq. (2) gives a fairly satisfactory correlation in the present case) to define a transition Reynolds number  $Re \propto (Gr^3/Pr)^n$  where  $n \propto 1/8$ . A similar result can be obtained along the lines used by Anderson if it is stated that at transition the shear stress existing with turbulent flow will equal the maximum shear existing with free convection from the stationary cylinder. The representation of figure 6 tests this kind of relation and there the results are shown not by points but by the Reynolds number range between the point of minimum Nusselt number and a Nusselt number located on the turbulent flow line. The range so specified depends to some extent on the closeness of successive points, and the character of the evaluation can be judged by comparing figure 6, where the Prandtl number magnitude is indicated, with the associated points on figure 4.

Figure 6 also contains Anderson's points and the range of Etemad's (ref. 2) results, the latter covering a limited range of abscissa values but showing no real trend in the transition Reynolds number. A "best fit" line is drawn through all the points for the prediction of the transition Reynolds number, giving the relation

$$Re_t = 4.7(Gr^3/Pr)^{0.137} \quad (5)$$

### Turbulent Flow

At Reynolds numbers greater than those specified by equation (5) the flow becomes turbulent and the upward components of velocity still necessary for the removal of heat occur at relatively larger distances from the cylinder. This diminishes the influence of free convection on the primary thermal resistance which is situated close to the cylinder surface for turbulent flow. The evaluation of the remaining free-convection effect is difficult; with air Etemad found effects after transition, while the results of Anderson and of Kays show a far less discernible influence. With oil, where the controlling resistance will be exactly at the cylinder surface, the effect is certainly anticipated to be small.

For a correlation alone, it is important first to test equation (3), the heat-transfer representation of Eisenberg's mass-transfer correlation (ref. 7). Figure 7(a) shows the result of this test and contains all data obtained above the transition Reynolds number and these, when compared with the curve for  $\frac{c_f}{2} \frac{ud}{v}$ , reveal departures of as much as 20 percent at high and low Reynolds numbers with better correspondence in the intermediate region. This does not much exceed the scatter of the mass-transfer results and indicates that, within the 20-percent limit, equation (3) serves to specify the present results.

In addition to the test of a correlation equation for Prandtl numbers of the order of those involved here, it is of interest to compare the test results with the prediction of an analogy calculation of the Karman type, a comparison already noted as having been successful with air. For high Prandtl numbers such a model must incorporate a turbulent transport effect which exists all the way to the wall in order to avoid excessively low predictions of the heat-transfer coefficient. Diessler (ref. 10) has achieved success in this regard for turbulent flow in pipes and the use of this model, considering only the region near the wall because of the large magnitude of the Prandtl number, relates the heat transfer to the shear coefficients in the following way:

$$\frac{hd}{k} = \frac{2n}{\pi} \sqrt{c_f} \frac{ud}{v} \left( \frac{\nu}{\alpha} \right)^{1/4} \quad (6)$$

Here the quantity  $n$  is empirical, being determined by Diessler as  $n = 0.124$  to insure an appropriate specification of the distribution of mean velocity near a pipe wall. Figure 7(b) shows the same results as figure 7(a) with the ordinate changed to  $\frac{hd}{k} \left( \frac{\alpha}{\nu} \right)^{1/4}$  in agreement with equation (6). The correlation of results is somewhat improved but these results depart considerably from the curve of equation (6) based on

$n = 0.124$ . The agreement appears better at high Reynolds numbers but at low Reynolds numbers the results are high by a factor of 2. No simple alteration of the quantity  $n$  will produce marked improvement, nor would such an alteration be essentially justifiable. It may only be concluded that for high Prandtl numbers the analogy prediction for the case of the rotating cylinder is quite inferior to that for turbulent flow in a pipe.

## DISCUSSION

In the foregoing presentation of results for the heat transfer, the flow was not considered specifically though it was taken implicitly as two dimensional. This was not really true in the present apparatus nor was it so in the devices used to obtain the results for air which are already available for this kind of system. These results for air, obtained from cylinders of different length-to-diameter ratio, appear to be reasonably independent of the geometrical form of the apparatus so that distortions from the two-dimensional flow would seem to have a minor effect on the heat transfer in the central position of the cylinder. It is useful, however, to consider some aspects of the flow which might bear on the heat-transfer behavior.

A feature of the isothermal friction coefficient as presented by Theodorsen is the termination of laminar flow at a Reynolds number of 70, followed by a gradual variation of the friction coefficient to a Reynolds number of 1,000, after which its character conforms to expectation for a fully developed turbulent flow. But because of the absence of any abrupt variation in the intermediate region, the flow is also considered as being fully turbulent. Before these results were available, Richardson (ref. 11) analyzed mean-velocity profiles near a rotating cylinder and concluded that at a Reynolds number above 70 the flow near the cylinder was turbulent. Also, since his observations indicated distributions of the laminar type at distances from the cylinder when the cylinder Reynolds number exceeded 70 which occurred in regions where the local Reynolds number  $ur/\nu$  was less than 35, he proposed that his criterion be applied on a local basis. In a two-dimensional flow, however, the product of the shear stress and the square of the radius must be constant, and a consideration of the friction coefficients measured by Theodorsen indicates that a flow, once turbulent, could never achieve a local Reynolds number less than 35 at greater radii. While details of Richardson's apparatus were not given, his observations suggest that the traction on the stationary side walls may significantly change the shear distribution from a two-dimensional distribution.

In addition to the effect of the side walls, the cylinders used in this type of investigation did not all have uniformly heated surfaces.

Thus, as was true in the present case, the free-convection effects did not extend over the entire length of the cylinder. An experimental investigation of the effect of the side walls was made using the cylinder previously used by Etemad, wherein side walls of large lateral extent were moved inward first to enclose only the heated section of the cylinder and finally to enclose a center section only one diameter wide. No change in the results from those given by Etemad was found in either the free-convection or fully turbulent regime to lead to the conclusion that the effect of the side walls on the flow produced a negligible effect on the heat-transfer performance.

In addition to a distortion of the overall two-dimensional character of the flow there possibly exist small-scale axial velocity components, as would be produced by vortical motion due to instability. Such have been predicted and measured by Taylor for laminar flow between concentric cylinders of similar radii, but no such solution for a very large radius ratio is available and for a single cylinder in an infinite medium the laminar flow is stable. A velocity distribution of the turbulent type is unstable, and, with slight distortion, the laminar distribution may be also, so that with the rotating cylinder there is a strong possibility of secondary flow. Etemad (ref. 2) provided interferometer photographs indicating an axial nonuniformity of the density field, possibly due to such secondary flow, which existed up to Reynolds numbers of the order of  $10^4$ . The existence of such a flow, which cannot be proved in the present experiments with oil, might provide the added heat transfer necessary to produce the difference between the actual and predicted heat transfer as obtained by analogy calculations and shown in figure 7(b).

## CONCLUSIONS

The effect of rotation on the free convection from a horizontal cylinder has been examined with oil as the fluid to secure results at Prandtl numbers from about 130 to 660 for comparison with available results with air. The following conclusions were drawn from this investigation:

1. In the free-convection region, where the flow is laminar, the effect of rotation depends on the Prandtl number and the Reynolds number, and a representation of the results has been found which produces a fair correlation and is at the same time in agreement with the results for air.

2. For turbulent flow a fair correlation is achieved through the representation proposed by Eisenberg for even higher Prandtl numbers. Analogy predictions do not give good agreement unless there is added

arbitrarily to the theory some postulate of an increased transport effect near the wall above that which is postulated by Diessler in his analysis.

University of California,  
Berkeley, Calif., February 17, 1958.

## APPENDIX A

## OPERATION WITH WATER

After the completion of the measurement of heat transfer from a cylinder rotating in oil the oil was removed, the system was cleaned, and once-distilled water was introduced. The electrical conductivity of the water was finite but the resistance from cylinder surface to the tank walls was satisfactorily high so that electrical leakage in that direction could be ignored. The water also provided a parallel conducting path along the ribbon, which diminished slightly the total resistance between the terminals thereof, but measurement of the resistance of the ribbon between its terminals on the cylinder both in air and submerged in water revealed the resistance to be the same in both cases within  $\pm 1$  percent. All electrical leakage therefore could be ignored and the results should be directly comparable with those for oil. The results obtained are of limited scope and are shown in figure 8.

Because of time limitations, free-convection results were not obtained with the cylinder held stationary, but rather with it having a low rotational speed of the order of 3 rpm, and the results for such an operation are shown on the inset of figure 8, where the Reynolds numbers are indicated. With Reynolds numbers below 1,000, there is excellent correspondence with equation (4); above  $Re = 1,000$ , the results are high. An altered effect of rotation on free convection can be visualized in this latter case, which has values of  $GrPr$  between  $10^8$  and  $10^9$ , which is the region where the initiation of turbulent free-convection flow is expected. The high values are attributed to such an effect.

Figure 8 shows the result of increasing rotative speed on the heat transfer and contains also, for reference, some shaded points which represent the results for oil shown in figure 7(a). The points for the lower Grashof numbers show absolutely no effect of rotation on the heat transfer until a Reynolds number of 3,000, and they agree exactly with equation (4). At higher Reynolds numbers rotational turbulent flow occurs and a fair coincidence with the trend of the oil results is attained, though the results are 20 percent higher than would be predicted by equation (3). The heat-transfer coefficients for the higher Grashof number are above the prediction of equation (4), apparently because of the turbulent free-convection flow as noted previously. At a Reynolds number of 4,500 agreement again occurs, though this is also near the region at which turbulent rotational flow occurs. Here there is some effect of rotation on free convection but certainly not in the context of figure 5, which considers only laminar free-convection flow. At Reynolds numbers above 4,500 the results agree with those for the lower Grashof number.

These results for water, at least those in the lower Grashof number range, agree completely with the results given in figure 5. The abscissa of that figure would be of the order of 2.5 at the point where transition to turbulent rotational flow occurs, and no effect of rotation on free convection would be predicted thereby. This is indeed true of the experimental results. The point of transition also agrees with the prediction of equation (5), so this can be used to indicate the termination of laminar free-convection flow with water to the same extent as that shown for oil and air in figure 6.



## APPENDIX B

## HEAT TRANSFER FROM VERTICAL CYLINDERS

An adjunct to the investigation of heat transfer from a horizontal cylinder rotating in oil was the determination of heat transfer from a vertical cylinder in air. In the main this determination was made to obtain results for this altered cylinder position but it served also as part of a program to experience the personnel in obtaining data before the cylinder described in the main text of this paper became available. Etemad's original Bakelite cylinder was used. It is also 2.50 inches in diameter and heated with a Nichrome ribbon which is 1 inch wide and 0.002 inch thick and wound helically around the cylinder.

A primary feature of vertical operation is the relative independence of the free-convection motion from the rotation of the cylinder. Examination of the equations of motion reveals that for constant properties this would be exactly so and the relatively small property variation in the case of free convection with air makes the constant-property deduction applicable. Nevertheless, the results already presented for the horizontal cylinder show that results from operation in air are inadequate for a relative appraisal of the absence of such interaction, for even with horizontal operation the gross free-convection effect is scarcely dependent upon rotation. Thus with air the results for vertical operation are similar to those for horizontal operation insofar as the effects of rotation are concerned.

Figure 9 shows the results achieved with a stationary vertical cylinder in terms of the local Nusselt number as a function of the Grashof number, the Nusselt number being for the center of the heated length. Because of the large helix angle produced by the 1-inch-wide ribbon on this cylinder, there existed a substantial difference in heated length as measured along the cylinder generator to the two thermocouples which were both in the same horizontal position. By the same token, it cannot be said that the free-convection flow was symmetrical with respect to the center line. These and other effects may account for the discrepancy between the results of figure 9 and the predictions shown there. The predictions are of themselves approximate, being obtained from the solution for constant heat flux on a vertical plate according to reference 12 and corrected for curvature according to the results in reference 13 for an isothermal vertical cylinder.

Figure 10 shows the effect of rotation on the heat transfer and has indicated upon it the Nusselt numbers  $\frac{hd}{k}$  corresponding to stationary operation as portrayed in figure 9. The effect of rotation on the free

convection is seen to be insignificant until a Reynolds number of the order of 1,000 is attained, after which there is a rapid elimination of the free-convection effect. One of Etemad's curves for horizontal operation at a similar value of the Grashof number is included to show the resemblance of the results. In the turbulent region the performance of the vertical cylinder is substantially the same as if it were horizontal and equation (1) serves to specify the heat-transfer coefficient. The insensitivity to cylinder position in this region is expected because of the dominating influence of cylinder rotation on the heat-transfer performance.

## REFERENCES

1. Anderson, J. T., and Saunders, O. A.: Convection From an Isolated Heated Horizontal Cylinder Rotating About Its Axis. Proc. Roy. Soc. (London), ser. A, vol. 217, no. 1131, May 21, 1953, pp. 555-562.
2. Etemad, G. A.: Free-Convection Heat Transfer From a Rotating Horizontal Cylinder to Ambient Air With Interferometric Study of Flow. Trans. ASME, vol. 77, no. 8, 1955, pp. 1283-1289.
3. Kays, W. M., and Bjorklund, I. S.: Heat Transfer From Rotating Bodies - Part I. The Horizontal Cylinder in an Infinite Environment. Tech. Rep. No. 27, Contract N6-onr-25106, Office of Naval Res. and Dept. Mech. Eng., Stanford Univ., 1955.
4. Dropkin, David, and Carmi, Arie: Natural-Convection Heat Transfer From a Horizontal Cylinder Rotating in Air. Trans. ASME, vol. 79, no. 4, 1957, pp. 741-749.
5. Theodorsen, Theodore, and Regier, Arthur: Experiments on Drag of Revolving Disks, Cylinders, and Streamline Rods at High Speeds. NACA Rep. 793, 1944.
6. Mayhew, Y. H.: The Reynolds Analogy Applied to a Cylinder Rotating in Air. Jour. R.A.S., vol. 58, no. 518, Mar. 1954, pp. 205-208.
7. Eisenberg, M., Tobias, C. W., and Wilke, C. R.: Mass Transfer at Rotating Cylinders. Chem. Eng. Prog., vol. 21, Symposium Ser. no. 16, 1955.
8. McAdams, W. A.: Heat Transmission. Third ed., McGraw-Hill Book Co., Inc., 1954.
9. Levy, S.: Integral Methods in Natural Convection Flow. Jour. Appl. Mech., vol. 22, no. 4, Dec. 1955, pp. 515-522.
10. Diessler, Robert G.: Analysis of Turbulent Heat Transfer, Mass Transfer, and Friction in Smooth Tubes at High Prandtl and Schmidt Numbers. NACA Rep. 1210, 1955. (Supersedes NACA TN 3145.)
11. Richardson, E. G.: Circulation Due to a Cylinder Rotating in a Viscous Fluid. Phil. Mag., vol. 11, 1931.
12. Sparrow, E. G., and Gregg, J. L.: Laminar Free Convection From a Vertical Plate With Uniform Surface Heat Flux. Trans. ASME, vol. 78, no. 2, 1956, pp. 435-440.

18.

13. Sparrow, E. G., and Gregg, J. L.: Laminar-Free-Convection Heat Transfer From the Outer Surface of a Vertical Circular Cylinder. Trans. ASME, vol. 78, no. 8, 1956, pp. 1823-1829.

TABLE I.- SUMMARY OF RESULTS

| Run                       | Prandtl<br>number,<br>$\nu/\alpha$ | Reynolds<br>number,<br>$ud/\nu$ | Grashof<br>number,<br>Gr | Nusselt<br>number,<br>$hd/k$ | Heat-transfer<br>coefficient,<br>h | $\Delta t$ , °F | $t_{\infty}$ , °F | Rotative<br>speed,<br>rpm |
|---------------------------|------------------------------------|---------------------------------|--------------------------|------------------------------|------------------------------------|-----------------|-------------------|---------------------------|
| Stationary cylinder - oil |                                    |                                 |                          |                              |                                    |                 |                   |                           |
| 33                        | 195                                | -----                           | $11.3 \times 10^4$       | 39.1                         | 13.6                               | 20.5            | 144               | -----                     |
| 36                        | 290                                | -----                           | 4.89                     | 31.2                         | 11.1                               | 20.8            | 121               | -----                     |
| 37                        | 665                                | -----                           | .885                     | 25.0                         | 9.22                               | 21.3            | 84                | -----                     |
| 65                        | 430                                | -----                           | 5.22                     | 37.3                         | 13.5                               | 50.2            | 88                | -----                     |
| 75                        | 166                                | -----                           | 28                       | 49.5                         | 17.0                               | 34.1            | 149               | -----                     |
| 79                        | 318                                | -----                           | 15                       | 47.0                         | 16.8                               | 79.6            | 127               | -----                     |
| Rotating cylinder - oil   |                                    |                                 |                          |                              |                                    |                 |                   |                           |
| 9                         | 660                                | 44                              | $0.865 \times 10^4$      | 12.7                         | 4.68                               | 21.1            | 84.5              | 10.5                      |
| 11                        | 676                                | 118                             | .714                     | 26.2                         | 9.67                               | 18.8            | 84.2              | 30                        |
| 12                        | 676                                | 161                             | .795                     | 31.4                         | 11.6                               | 20.4            | 83.9              | 40                        |
| 13                        | 630                                | 70                              | 1.0                      | 11.5                         | 4.21                               | 21.9            | 86.4              | 16                        |
| 14                        | 630                                | 100                             | .999                     | 22.8                         | 8.37                               | 21.7            | 86.2              | 23                        |
| 15                        | 650                                | 218                             | .876                     | 38.6                         | 14.2                               | 20.4            | 85.6              | 52                        |
| 16                        | 660                                | 256                             | .853                     | 41.8                         | 15.4                               | 20.8            | 84.7              | 62                        |
| 17                        | 660                                | 430                             | .849                     | 58.9                         | 21.7                               | 20.7            | 84.6              | 102                       |
| 18                        | 676                                | 1,015                           | .823                     | 102                          | 37.8                               | 20.1            | 83.7              | 252                       |
| 19                        | 610                                | 2,175                           | 1.02                     | 167                          | 61.5                               | 21.3            | 87.3              | 488                       |
| 20                        | 600                                | 4,580                           | .939                     | 308                          | 113                                | 18.4            | 90                | 996                       |
| 21                        | 194                                | 39.0                            | 12                       | 186                          | 64.7                               | 21.3            | 144               | 254                       |
| 22                        | 194                                | 7,790                           | 12                       | 310                          | 108                                | 21.2            | 144               | 506                       |
| 23                        | 190                                | 15,590                          | 11                       | 526                          | 183                                | 19.8            | 146               | 999                       |
| 24                        | 190                                | 166                             | 12                       | 26.3                         | 9.15                               | 20.7            | 146               | 10.5                      |
| 25                        | 188                                | 317                             | 12                       | 39.5                         | 13.7                               | 22.0            | 146               | 19.8                      |
| 26                        | 190                                | 474                             | 11                       | 53.6                         | 18.6                               | 19.3            | 147               | 30                        |
| 27                        | 190                                | 624                             | 13                       | 62.0                         | 21.5                               | 23.6            | 144               | 40                        |
| 28                        | 190                                | 811                             | 13                       | 72.4                         | 25.1                               | 23.8            | 144               | 52                        |
| 29                        | 190                                | 936                             | 14                       | 78.0                         | 27.1                               | 24.5            | 144               | 60                        |
| 30                        | 190                                | 1,575                           | 13                       | 105                          | 36.4                               | 24.0            | 144               | 101                       |
| 31                        | 193                                | 178                             | 12                       | 26.1                         | 9.07                               | 20.3            | 145               | 11.5                      |
| 32                        | 194                                | 196                             | 11                       | 26.4                         | 9.21                               | 20.0            | 144               | 13.0                      |
| 34                        | 184                                | 80.5                            | 16                       | 36.9                         | 12.8                               | 26.2            | 145               | 5                         |
| 35                        | 184                                | 32.2                            | 15                       | 39.8                         | 13.8                               | 24.2            | 146               | 2                         |
| 38                        | 650                                | 16.8                            | 1.023                    | 22.2                         | 8.20                               | 23.8            | 83.8              | 4                         |
| 39                        | 650                                | 1.0                             | .876                     | 25.3                         | 9.33                               | 21.1            | 84.5              | 1/4                       |
| 40                        | 315                                | 200                             | 13                       | 25.6                         | 9.13                               | 64.6            | 95.8              | 22                        |
| 41                        | 410                                | 136                             | 6.6                      | 20.4                         | 7.41                               | 58.3            | 86.5              | 20                        |
| 42                        | 420                                | 191                             | 6.0                      | 21.8                         | 7.90                               | 56.6            | 85.5              | 29                        |
| 43                        | 275                                | 100                             | 6.12                     | 22.4                         | 7.97                               | 240             | 122               | 10                        |
| 44                        | 275                                | 191                             | 6.02                     | 31.2                         | 11.1                               | 23.6            | 122               | 19                        |
| 45                        | 275                                | 501                             | 6.07                     | 52.8                         | 18.7                               | 23.8            | 122               | 50                        |
| 46                        | 275                                | 1,000                           | 5.71                     | 84.5                         | 30.0                               | 22.4            | 123               | 100                       |
| 47                        | 275                                | 2,525                           | 5.28                     | 154                          | 54.6                               | 20.7            | 123               | 252                       |
| 48                        | 280                                | 5,040                           | 5.18                     | 252                          | 89.2                               | 20.3            | 124               | 494                       |
| 49                        | 295                                | 9,480                           | 4.17                     | 419                          | 149                                | 18.7            | 122               | 988                       |
| 50                        | 290                                | 39.6                            | 4.42                     | 29.2                         | 10.4                               | 18.8            | 122               | 4                         |
| 51                        | 295                                | 19.2                            | 4                        | 31.4                         | 11.2                               | 17.5            | 122               | 2                         |
| 52                        | 285                                | 70.0                            | 5.2                      | 25.4                         | 9.0                                | 21.6            | 122               | 7                         |
| 53                        | 650                                | 30                              | 1.01                     | 17.1                         | 6.30                               | 23.6            | 84.6              | 7.2                       |
| 54                        | 280                                | 160                             | 6.4                      | 21.6                         | 7.66                               | 25.8            | 121               | 15.5                      |
| 55                        | 410                                | 3,660                           | 5.5                      | 227                          | 82.3                               | 49.8            | 89.6              | 539                       |
| 56                        | 410                                | 6,940                           | 5.6                      | 352                          | 127                                | 48.2            | 91.3              | 1,005                     |
| 57                        | 400                                | 113                             | 6.0                      | 24.0                         | 8.67                               | 54.9            | 89.9              | 15.7                      |

TABLE I.- SUMMARY OF RESULTS - Concluded

| Run                       | Prandtl<br>number,<br>$\nu/\alpha$ | Reynolds<br>number,<br>$ud/\nu$ | Grashof<br>number,<br>Gr | Nusselt<br>number,<br>$hd/k$ | Heat-transfer<br>coefficient,<br>h | $\Delta t$ , °F | $t_{\infty}$ , °F | Rotative<br>speed,<br>rpm |
|---------------------------|------------------------------------|---------------------------------|--------------------------|------------------------------|------------------------------------|-----------------|-------------------|---------------------------|
| Rotating cylinder - oil   |                                    |                                 |                          |                              |                                    |                 |                   |                           |
| 59                        | 410                                | 319                             | $5.7 \times 10^4$        | 56.0                         | 20.4                               | 50              | 90.2              | 47                        |
| 60                        | 420                                | 1,060                           | 5.8                      | 98.0                         | 35.4                               | 51              | 88.9              | 156                       |
| 61                        | 430                                | 1,830                           | 5.2                      | 143                          | 51.9                               | 49.7            | 88.3              | 278                       |
| 62                        | 440                                | 65.0                            | 5.0                      | 28.2                         | 10.2                               | 51.8            | 86.0              | 10.3                      |
| 63                        | 440                                | 31.5                            | 4.9                      | 38.3                         | 13.9                               | 50.9            | 86.7              | 5.0                       |
| 64                        | 440                                | 13.4                            | 5.3                      | 37.0                         | 13.4                               | 52.8            | 86.5              | 2.1                       |
| 66                        | 140                                | 26.0                            | 42                       | 45.3                         | 15.4                               | 33.8            | 162               | 1.15                      |
| 67                        | 137                                | 53.3                            | 38                       | 50.8                         | 17.2                               | 30.1            | 164               | 2.35                      |
| 68                        | 135                                | 156                             | 41                       | 48.4                         | 16.4                               | 31.6            | 164               | 6.8                       |
| 69                        | 136                                | 284                             | 40                       | 37.8                         | 12.8                               | 31.7            | 164               | 12.5                      |
| 70                        | 300                                | 25.1                            | 18                       | 48.8                         | 17.4                               | 86.6            | 87                | 2.6                       |
| 71                        | 310                                | 56.0                            | 17                       | 50.3                         | 17.9                               | 83.7            | 86.7              | 5.9                       |
| 72                        | 310                                | 157                             | 17                       | 39.9                         | 14.8                               | 83.9            | 87.8              | 16.5                      |
| 73                        | 300                                | 285                             | 19                       | 27.9                         | 9.95                               | 90.9            | 84.8              | 30.0                      |
| 74                        | 300                                | 570                             | 18                       | 65.7                         | 23.4                               | 82.2            | 89                | 60.0                      |
| 76                        | 137                                | 352                             | 39                       | 39.6                         | 13.8                               | 30.7            | 164               | 15.3                      |
| 77                        | 137                                | 405                             | 41                       | 42.4                         | 14.5                               | 31.3            | 165               | 17.6                      |
| 78                        | 137                                | 448                             | 34                       | 46.0                         | 15.4                               | 29.3            | 165               | 19.5                      |
| Rotating cylinder - water |                                    |                                 |                          |                              |                                    |                 |                   |                           |
| 88                        | 4.86                               | 795                             | $2.17 \times 10^7$       | 52.8                         | 90.3                               | 20.4            | 86.6              | 2.7                       |
| 89                        | 4.90                               | 1,495                           | 2.15                     | 52.7                         | 90.4                               | 20.4            | 86.2              | 5.1                       |
| 90                        | 4.94                               | 3,035                           | 2.0                      | 54.0                         | 92.7                               | 19.8            | 85.8              | 10.4                      |
| 91                        | 4.94                               | 6,070                           | 2.0                      | 90.8                         | 156                                | 19.0            | 86.3              | 20.8                      |
| 92                        | 4.73                               | 14,700                          | 2.06                     | 144                          | 249                                | 18.4            | 89.3              | 49                        |
| 93                        | 4.56                               | 31,400                          | 2.6                      | 258                          | 447                                | 20.6            | 91.8              | 101                       |
| 94                        | 4.32                               | 76,600                          | 3.2                      | 462                          | 807                                | 19.9            | 98.3              | 231                       |
| 95                        | 5.34                               | 4,380                           | 1.9                      | 69.5                         | 118                                | 21.2            | 80.0              | 15.9                      |
| 96                        | 5.01                               | 100,000                         | 1.6                      | 564                          | 969                                | 16.0            | 87.2              | 348                       |
| 97                        | 5.65                               | 5,950                           | 0.84                     | 78.3                         | 133                                | 9.5             | 85.7              | 21.6                      |
| 98                        | 4.6                                | 6,000                           | 3.5                      | 79.2                         | 137                                | 28.8            | 87                | 20                        |
| 99                        | 4.82                               | 29,600                          | 2.4                      | 232                          | 400                                | 22.5            | 86.5              | 100                       |
| 100                       | 4.44                               | 10,700                          | 2.5                      | 150                          | 260                                | 17.7            | 95.8              | 52.4                      |
| 101                       | 3.56                               | 41,500                          | 5.3                      | 255                          | 456                                | 19.7            | 117               | 104                       |
| 102                       | 3.27                               | 22,200                          | 5.3                      | 162                          | 293                                | 17.0            | 1,260             | 52.4                      |
| 103                       | 3.27                               | 9,450                           | 5.3                      | 92.0                         | 166                                | 15.7            | 127               | 22.3                      |
| 104                       | 3.14                               | 6,630                           | 5.8                      | 69.6                         | 126                                | 20.7            | 127               | 15.2                      |
| 105                       | 3.18                               | 4,450                           | 5.4                      | 64.0                         | 116                                | 16.5            | 128               | 10.3                      |
| 106                       | 3.17                               | 2,450                           | 4.5                      | 75.0                         | 136                                | 14.0            | 130               | 5.65                      |
| 107                       | 2.98                               | 1,260                           | 4.9                      | 77.0                         | 140                                | 13.5            | 135               | 2.80                      |
| 108                       | 5.58                               | 762                             | 1.7                      | 50.6                         | 85.7                               | 21.7            | 76.3              | 2.87                      |
| 109                       | 4.89                               | 846                             | 2.2                      | 52.6                         | 90.4                               | 20.6            | 86.2              | 2.88                      |
| 110                       | 3.83                               | 1,080                           | 5.3                      | 66.3                         | 117                                | 22.4            | 109               | 2.88                      |
| 111                       | 3.02                               | 1,290                           | 6.5                      | 83.0                         | 151                                | 19.3            | 131               | 2.90                      |

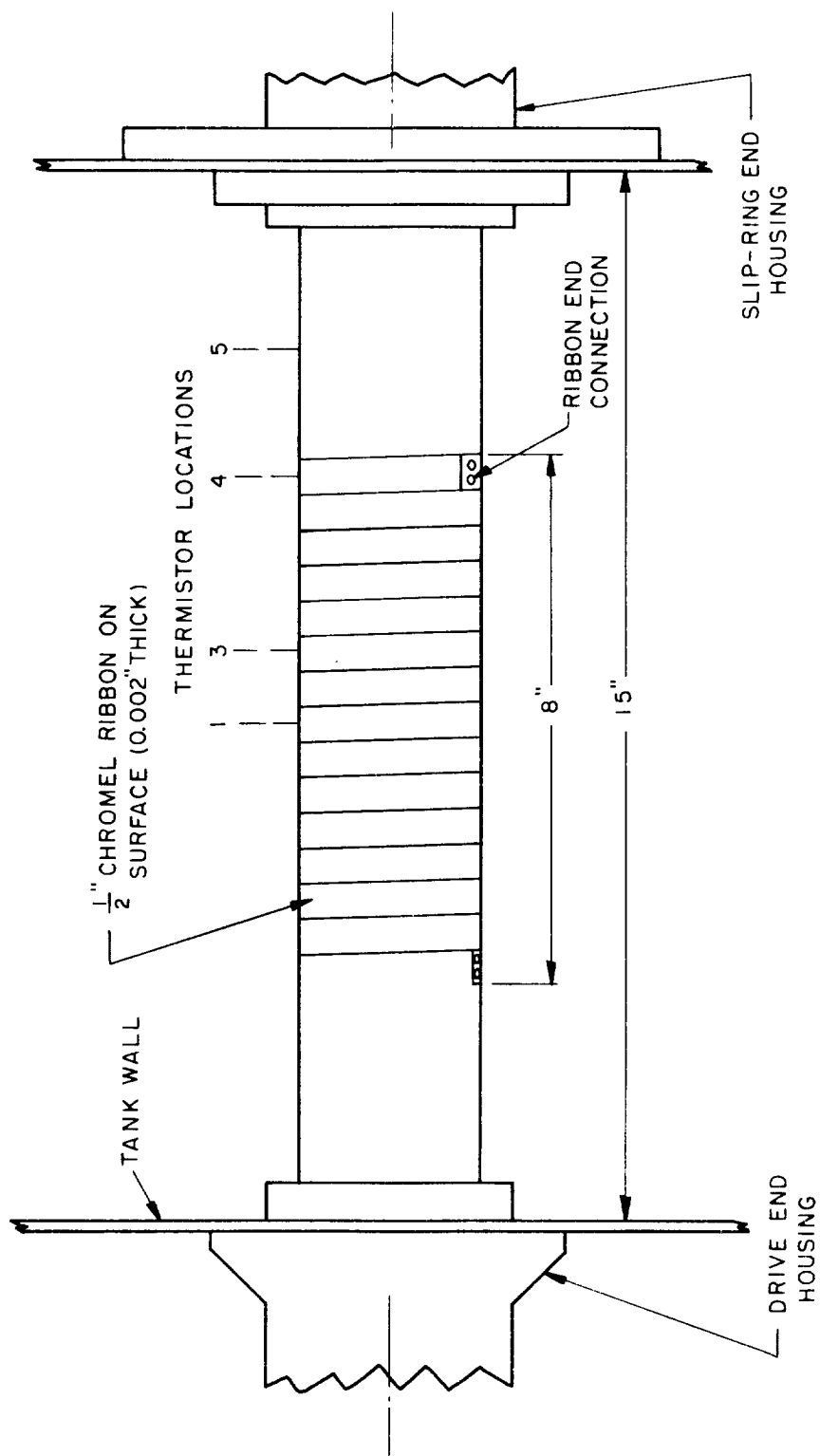


Figure 1.- Sketch showing elevation of cylinder in tank.

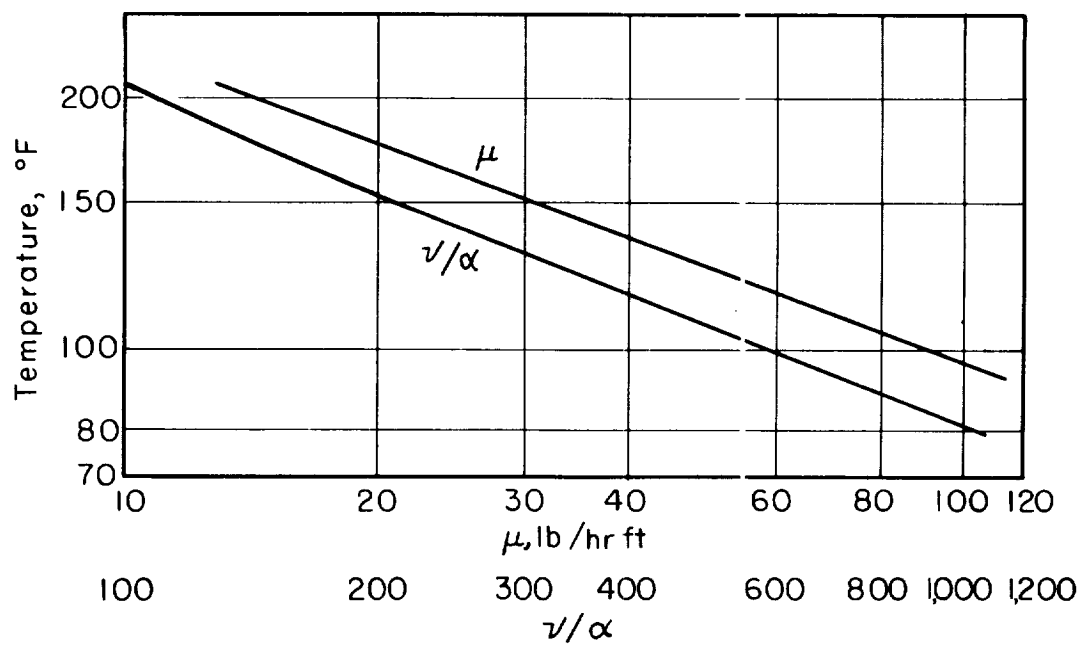
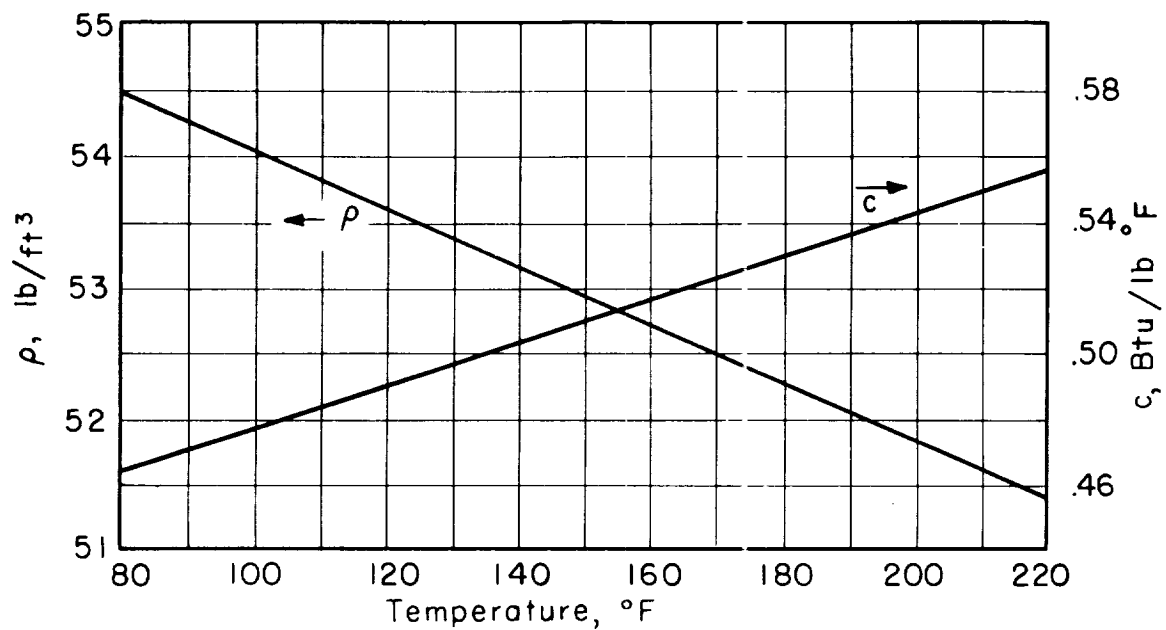


Figure 2.- Properties of oil used in experiments.



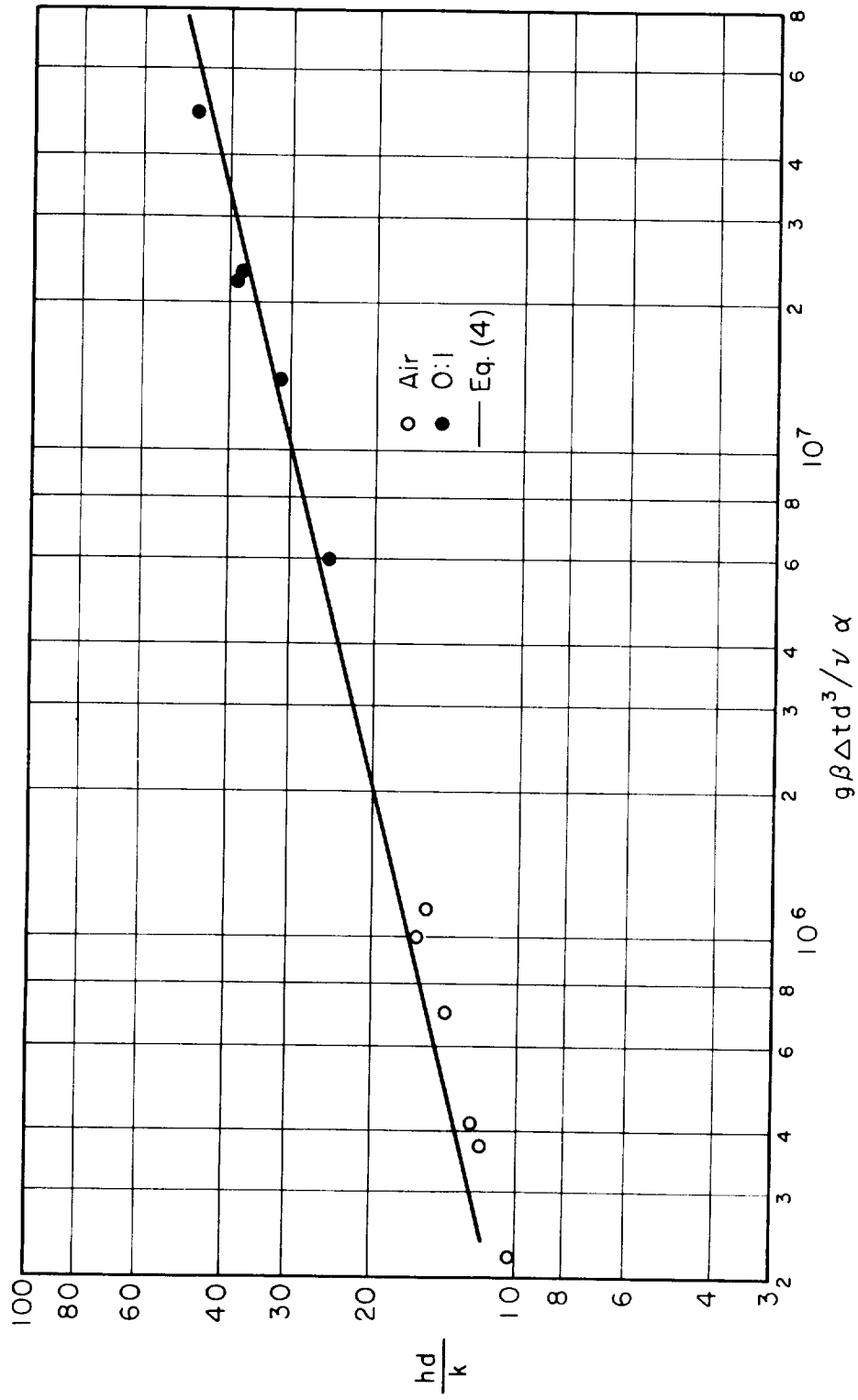


Figure 3.- Free-convection performance of stationary cylinder.

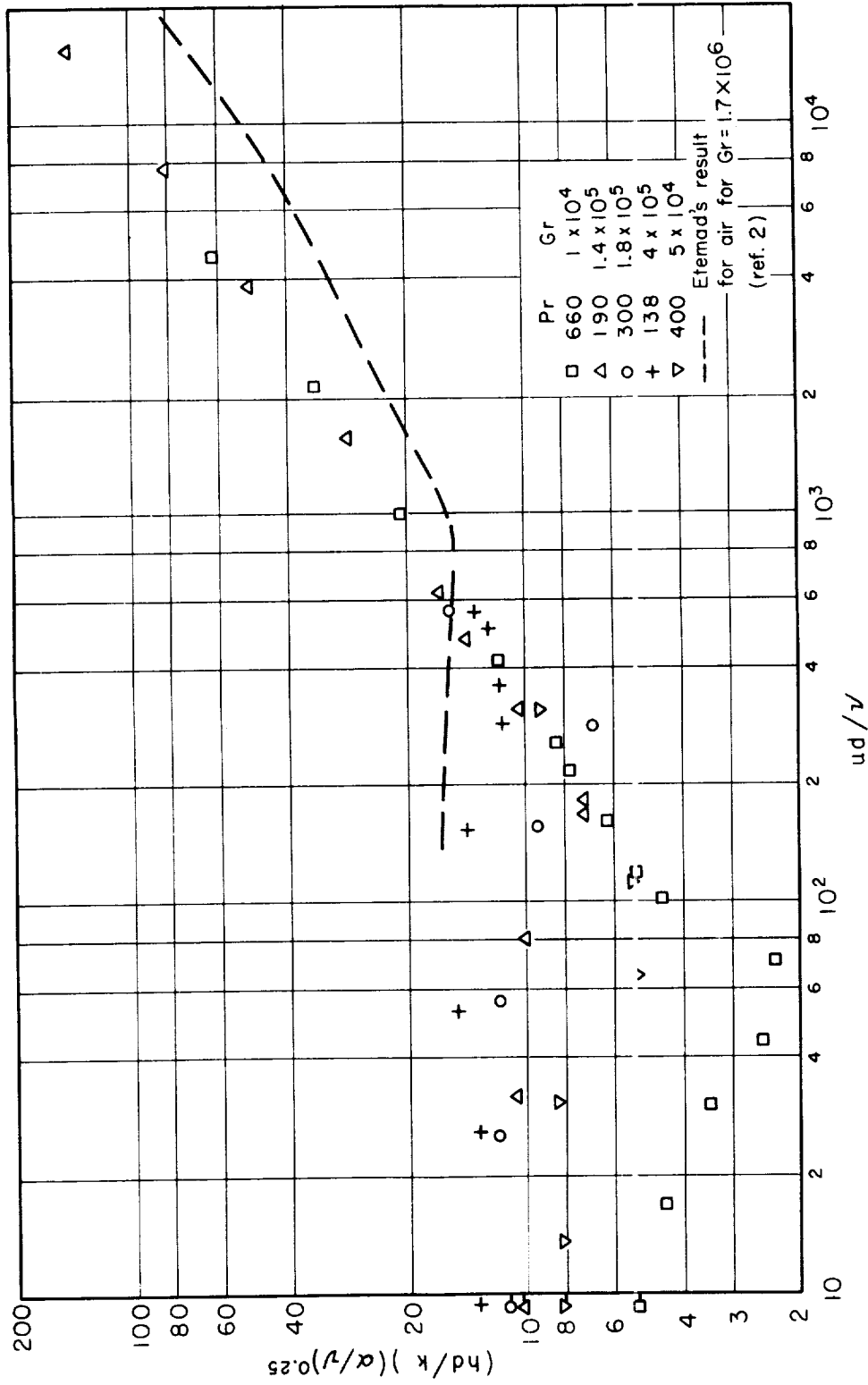


Figure 4.- Heat transfer with rotation. Points on ordinate line are predictions from equation (4) for Grashof and Prandtl number magnitudes associated with particular sets of points.

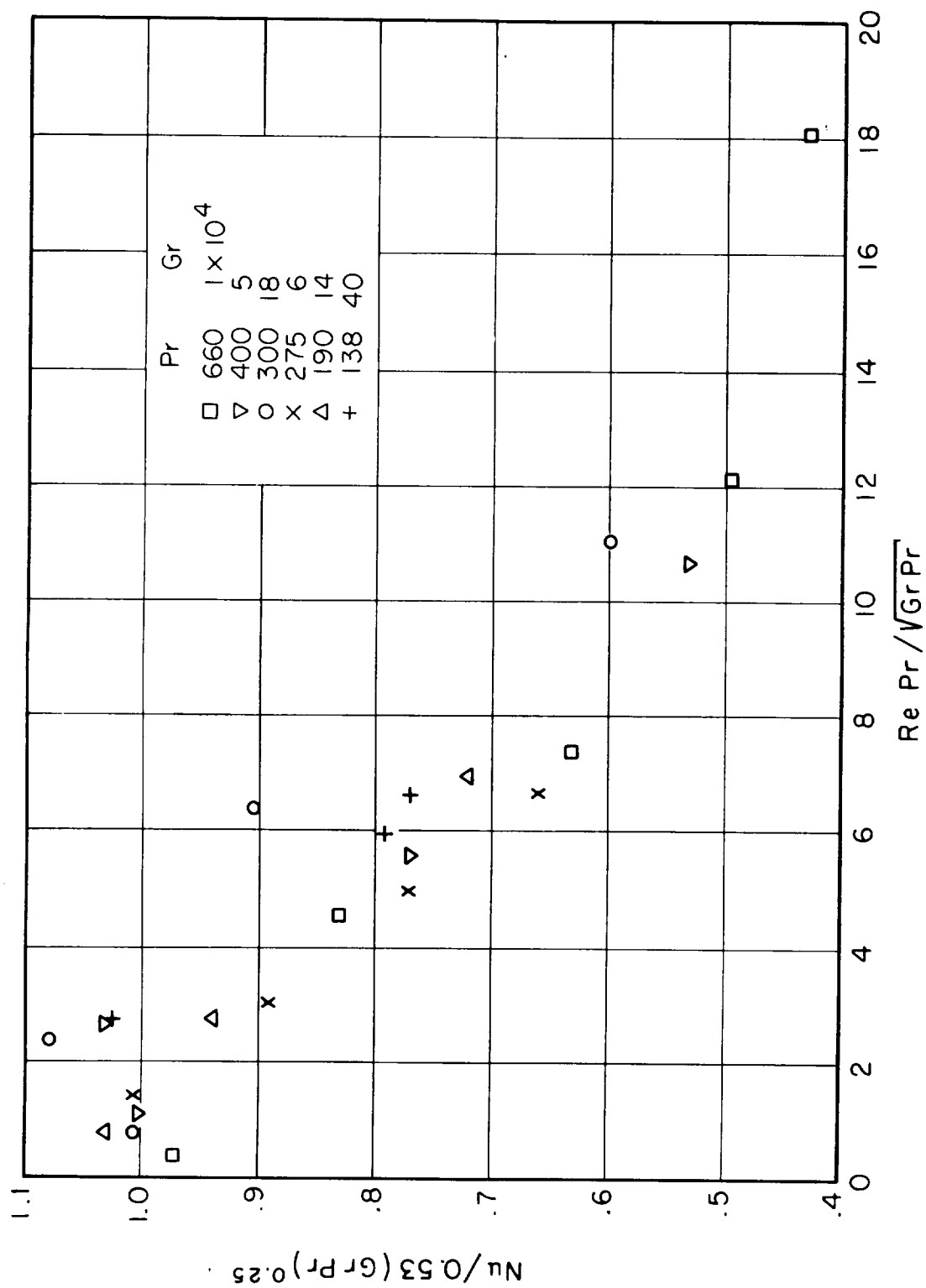


Figure 5.- Effect of rotation on free-convection performance.

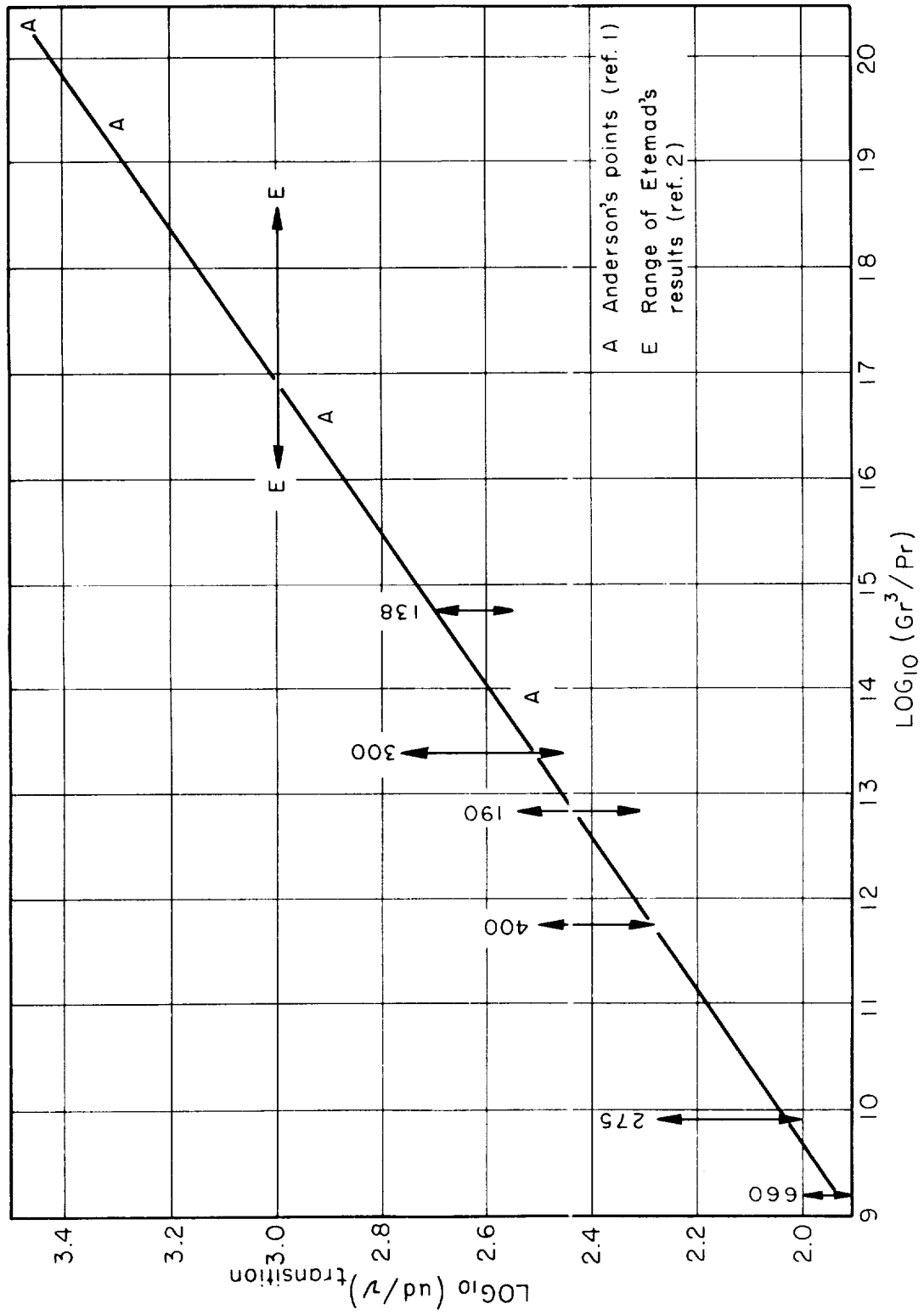
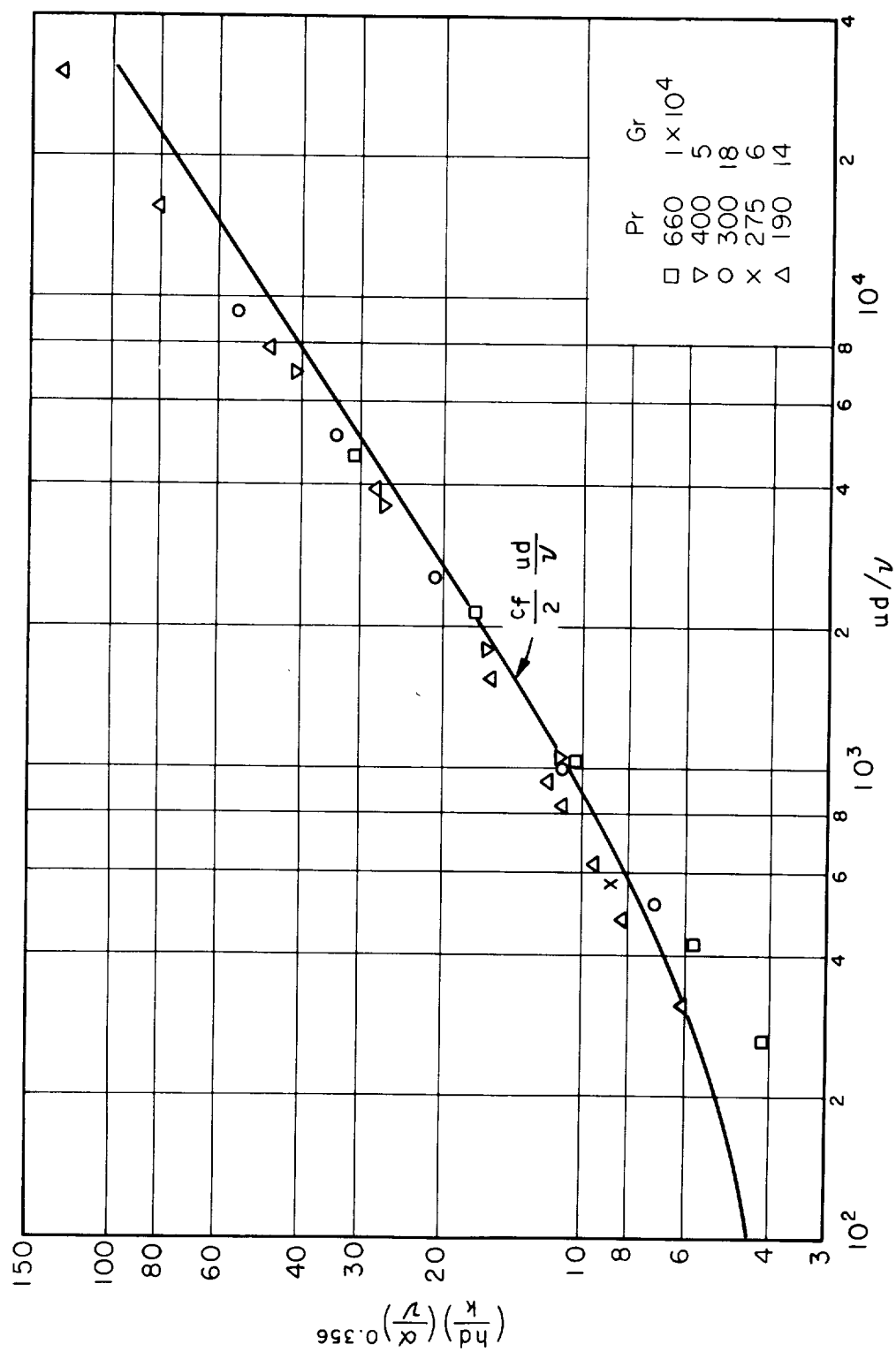
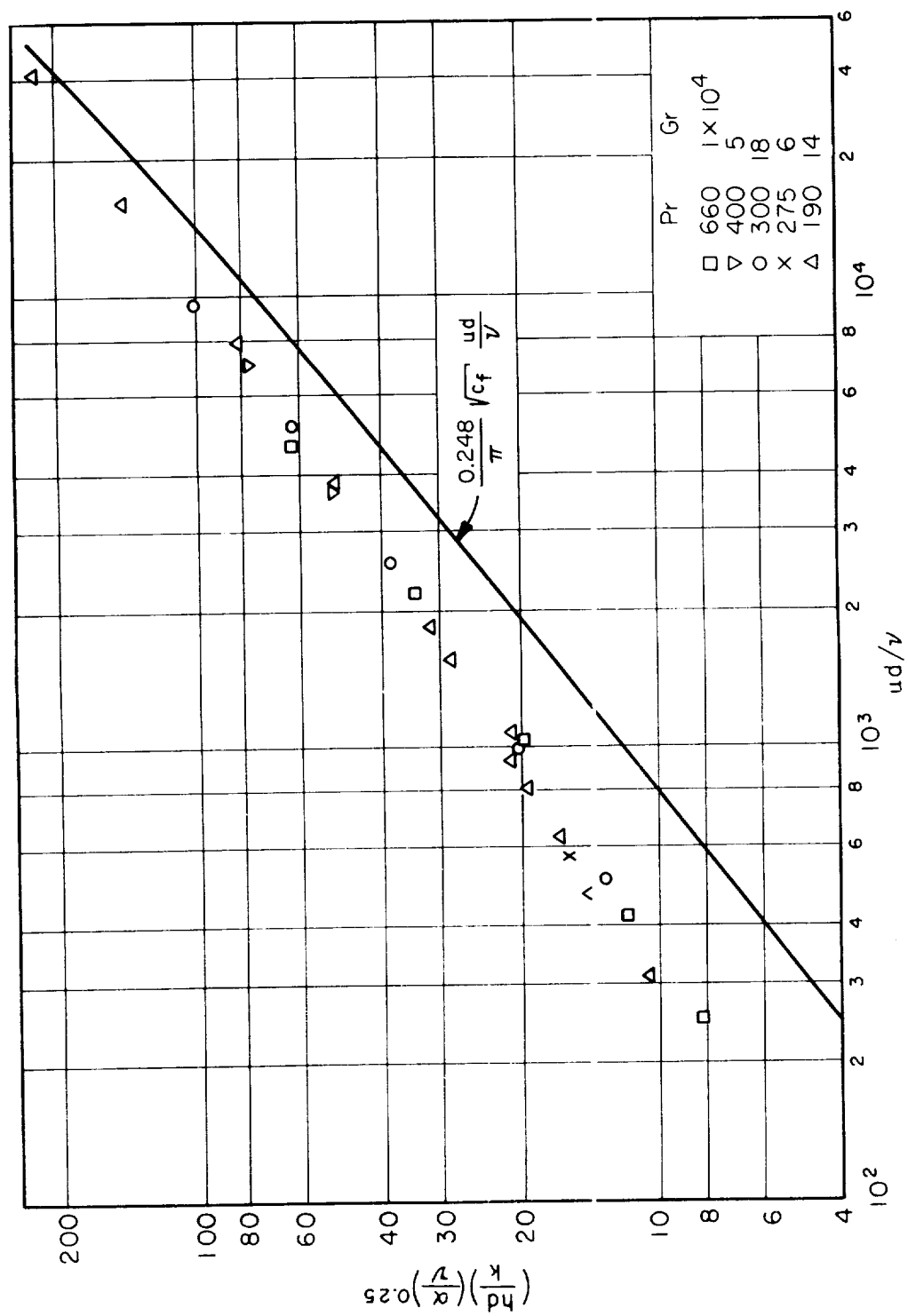


Figure 6.- Reynolds numbers for transition to turbulent flow.



(a) Representation in accordance with equation (3).

Figure 7.- Heat transfer with turbulent flow.



(b) Representation in accordance with equation (6).

Figure 7.- Concluded.

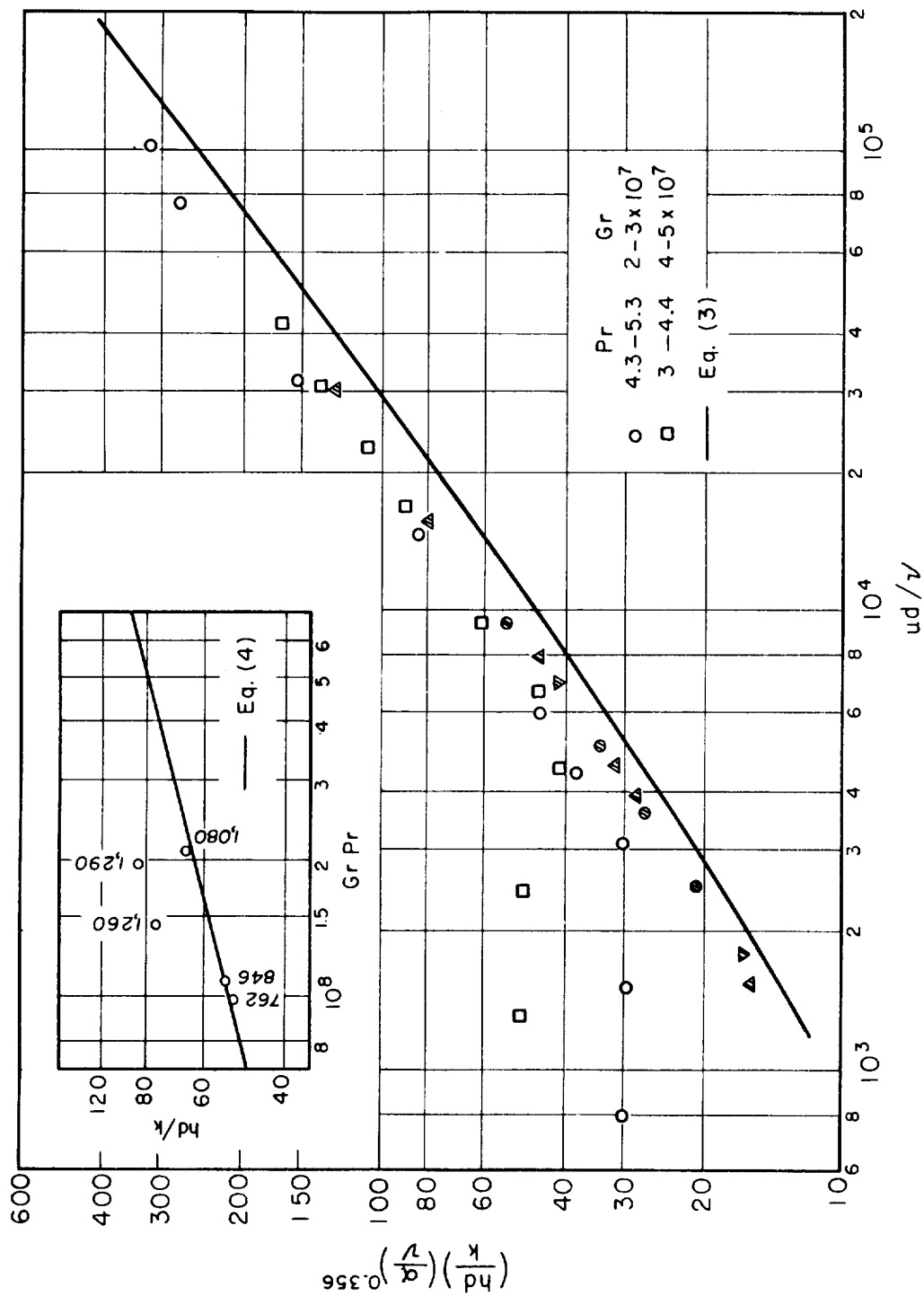


Figure 8.- Heat transfer with rotation in water. Inset shows performance at very low speed approximating stationary conditions. Reynolds numbers are indicated for individual points. Shaded points are from figure 7(a) for results with oil.

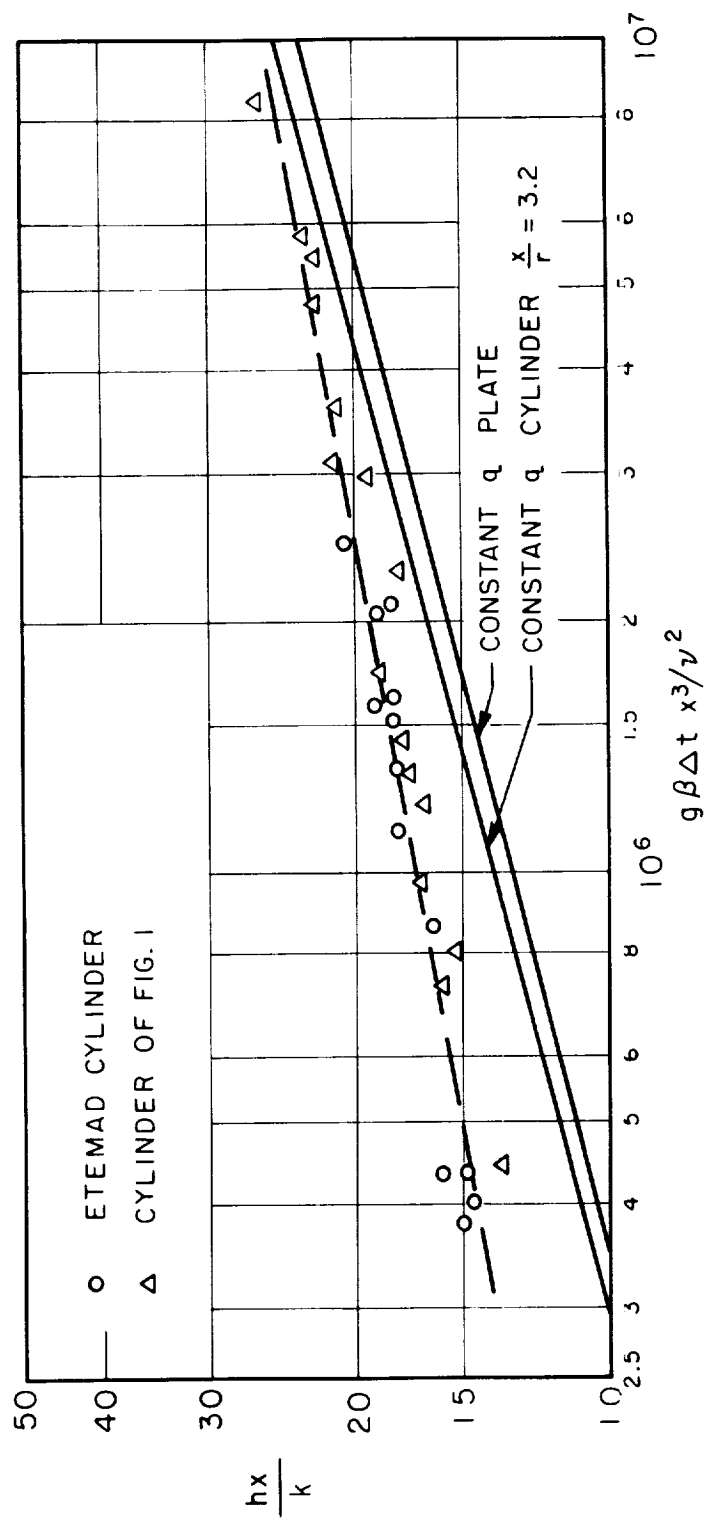


Figure 9.- Heat-transfer results from stationary cylinder with vertical axis. Solid curves are predictions for constant heat rate by Sparrow (refs. 12 and 13).  $\nu/\alpha = 0.70$ .



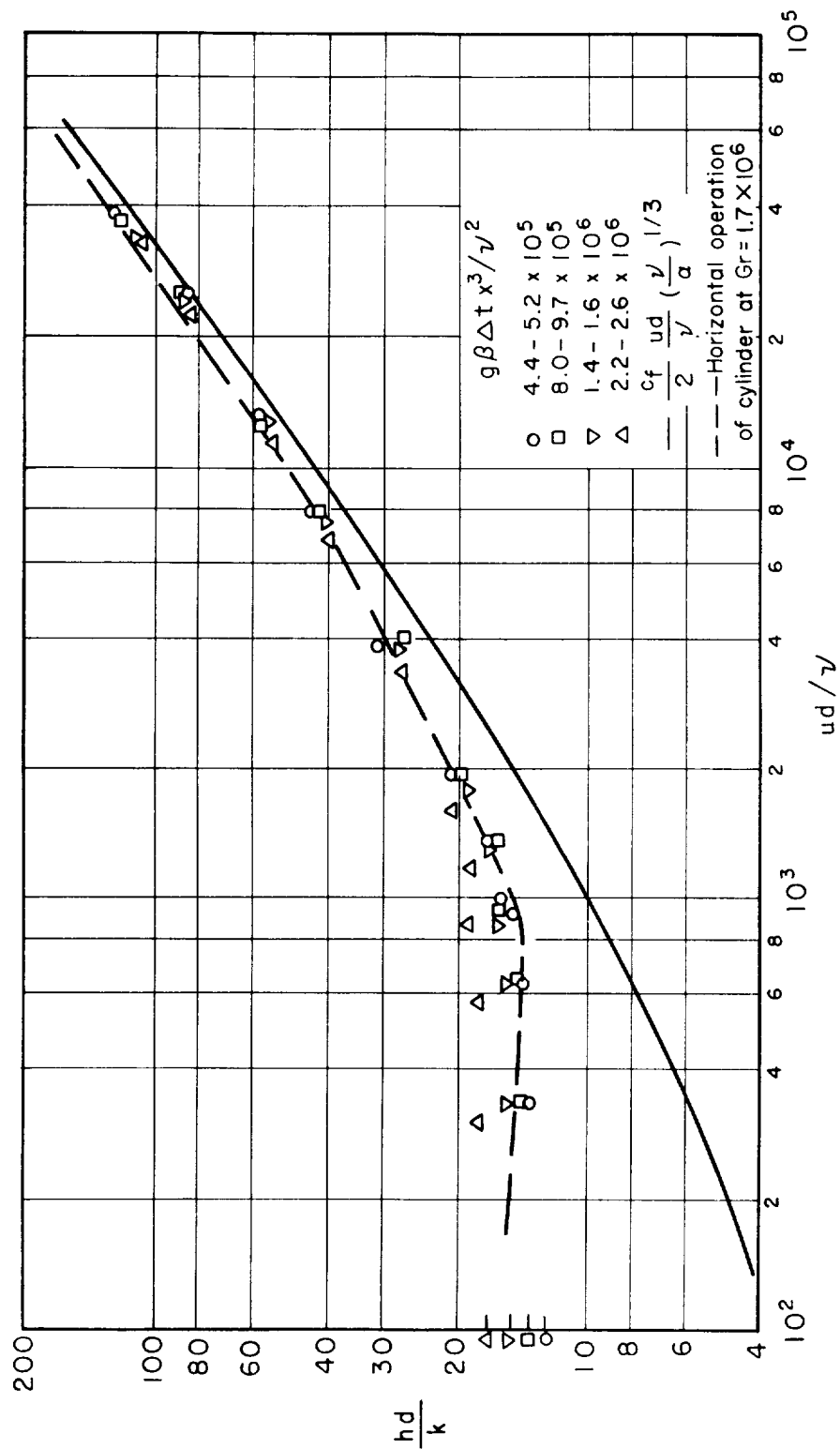


Figure 10.- Heat transfer from Etemad's cylinder operating vertically. Points on ordinate line are for stationary performance predicted from results of figure 9.

